Materials Letters 229 (2018) 364–367

Contents lists available at ScienceDirect

Materials Letters

journal homepage: www.elsevier.com/locate/mlblue

Structural and mechanical characterization of (TiZrNbHfTa)N/WN multilayered nitride coatings

A.A. Bagdasaryan [a,b,*], A.V. Pshyk [b], L.E. Coy [b], M. Kempiński [b,c], A.D. Pogrebnjak [a], V.M. Beresnev [d], S. Jurga [b]

[a] Sumy State University, 2, Rymsky Korsakov Str., 40007 Sumy, Ukraine
[b] NanoBioMedical Centre, Adam Mickiewicz University, 85, Umultowska Str., 61-614 Poznań, Poland
[c] Faculty of Physics, Adam Mickiewicz University, Umultowska 85, 61-614 Poznań, Poland
[d] Kharkiv National University, Svobody Sq., 4, 61022 Kharkiv, Ukraine

ARTICLE INFO

Article history:
Received 19 April 2018
Received in revised form 2 July 2018
Accepted 11 July 2018
Available online 11 July 2018

Keywords:
Multilayer structure
Chemical bonding
Solid solution
Mechanical properties

ABSTRACT

The (TiZrNbHfTa)N/WN multicomponent coatings were deposited by vacuum arc evaporation under different substrate bias (−90 and −280 V). X-ray photoelectron spectroscopy was used for analyzing of complex composition of investigated coatings by reflecting of atomic scale chemical interactions. The structural investigations showed the formation of a simple disordered solid solution in (TiZrNbHfTa)N layer, β-W_2N phase in WN layer with fcc crystal structure and highly disordered bcc (1 1 0) and (2 2 0) -oriented high-entropy alloy phases, regardless of the applied bias potential. It was shown that with increasing of substrate bias from −90 to −280 V, there is a slight decrease of hardness from 34 to 31 GPa and increase of Young's modulus from 325 to 337 GPa, which can be explained by annihilation of point defects and precipitation of relatively softer metallic phase.

1. Introduction

Nowadays, the development on new scientific approaches and new compositions of protective coatings is the paramount task of modern material science. Due to their broad range of physio-mechanical properties, like hardness, wear and corrosion resistivity, thermal resistance, electrical conductivity and adhesion to substrate, such materials can be used as protective or/and decorative coatings for enhancement of life time and providing the necessary properties for tools, machine parts and even medical devices [1].

One of the most promising approaches to the design of coatings is combination of layers of two or more different materials [2]. One of the successful manifestations of this approach is the multilayer nitride coatings of transition metals. It is well known, that nitrogen with transition metals can form mixed ion-metal-covalent bonds, which contributes to the creation of a strong and hard material. A large variety of preparation methods and vast composition range allowed to obtain coatings with excellent characteristics: TiN/VN [3], CrN/WN [4], TiVN/TiSiN [5] and etc. [6].

In the present work, we attempt to combine two types of thin layers of (TiZrNbHfTa)N and WN into the (TiZrNbHfTa)N/WN multicomponent coatings and investigated chemical bonds, structural-phase states and mechanical properties. Transition d-metals with a high negative enthalpy of nitride formation are used as constituent elements of the investigated systems for obtaining the highest functional properties of the coatings.

2. Experiments

The new (TiZrNbHfTa)N/WN multicomponent coatings deposited by vacuum arc evaporation. The surface was cleaned with ions of the evaporated material before deposition. The cleaning time was t = 10 min and the residual pressure in the chamber was $P = 7.4 \times 10^{-3}$ Pa (the deposition conditions are presented in the Table 1). The deposition was carried out from two sources (TiZrNbHfTa) and (W) with continuous rotation at a speed of 8 rpm. Steel discs (X12H9T steel) were used as substrates. The thickness of investigated coatings was near 9 ÷ 9.5 μm, layer period was 25 nm for (TiZrNbHfTa)N and 8 nm for WN layers.

The XPS data were obtained using the monochromatic Al Kα X-Ray source and Sphera II photoelectron energy analyzer (Scienta Omicron). All measurements were made in the ultra-high vacuum chamber at a pressure around 10^{-9} mbar. Spectra of core level lines were taken at 20 eV pass energy and resolution of 0.1 eV. The crystal structure was characterized by XRD PANalytical using filtered Cu-Kα radiation (1.5418 Å) with PIXcel 3D detector in Bragg-Brentano geometry. Diffractograms were recorded in continuous

* Corresponding author at: Sumy State University, 2, Rymsky Korsakov Str., 40007 Sumy, Ukraine.
E-mail address: artem.a.bagdasaryan@gmail.com (A.A. Bagdasaryan).

https://doi.org/10.1016/j.matlet.2018.07.048
0167-577X/

Table 1
Deposition parameters.

№	Sample	I, A	U_b, V	P_N, Pa
1	(TiZrNbHfTa)N/WN	190 100	−90	0.53
2	(TiZrNbHfTa)N/WN	190 100	−280	0.53

scanning mode at room temperature (300 K), with the 2θ ranging from 20.0° to −80.0° and scanning step was 0.006°. The nanoindentation tests were performed at room temperature on (TiZrNbTaHf)N/MoN coatings using Hysitron TriboIndenter TI 950 equipped with a Berkovich diamond tip TI-0039 under a maximum load at 10 mN. The measurements were repeated 10 times and analyzed by using the Oliver-Pharr methodology, which are described elsewhere [7].

3. Results and discussions

Fig. 1 shows XPS core-level spectra for the (TiZrNbHfTa)N/WN coating. The Nb 3d core-level spectrum (Fig. 1a) was deconvoluted into 3 spin-orbit doublets. The spin-orbit split $3d_{3/2}$ and $3d_{5/2}$ peaks at around 206.2 eV and 204.0 eV, respectively, correspond to the binding energy of NbN [8]. The spit-orbit split doublets at the high binding energy side of the spectrum are assigned to NbO_2 (204.8 eV ($3d_{5/2}$) and 208.2 eV($3d_{3/2}$) [8]) and Nb_2O_5 (207.0 eV ($3d_{5/2}$) and 209.5 eV($3d_{3/2}$)) phases. The Zr3d spectrum can be fitted with 2 spit-orbit split doublets, which are assigned to ZrN (179.8 eV ($3d_{5/2}$) and 181.7 eV($3d_{3/2}$) [9]) and ZrO_2 (182.3 eV ($3d_{5/2}$) and 184.4 eV($3d_{3/2}$) [8]) phases. The Ti 2p spectrum presents the asymmetrical Ti 2p3/2 and Ti 2p1/2 doublets, which match TiN (455.4 eV (2p3/2) and 461.2 eV (2p1/2)), TiON (456.7 eV (2p3/2) and 462.8 eV (2p1/2)) and TiO_2 (458.3 eV (2p3/2) and 464.1 eV (2p1/2) [10]) phases. The Hf 4f spectrum shows two Hf 4f5/2 and Hf 4f7/2 spin–orbit doublets, which could be attributed to HfN (15.2 eV (4f7/2) and 16.1 eV (4f5/2) [11]) and HfO_2 (16.8 eV (4f7/2) and 18.1 eV (4f5/2)) phases. Importantly, faint traces of W and Ta were detected in the coating, but the intensity of corresponding peaks was very low and overlap with the other peaks, which make them inappropriate for an accurate analysis.

The chemical composition of the deposited coatings were determined by EDX-method: Sample1: N – 22.52%, Hf – 3.73%, W – 25.09%, Zr – 12.56%, Nb – 11.45%, Ti – 20.14%; Ta – 4.51%; Sample 2: N – 18.37%, Hf – 2.8%, W – 42.35%, Zr – 7.84%, Nb – 7.32%, Ti – 17.56%, Ta – 3.76%. The non-stoichiometric composition can be associated with a low working gas pressure. A sharp decrease in the nitrogen concentration is obviously due to the sputtering of lighter atoms due to the high bias potential.

Disordered solid solution with a crystal lattice of the structural type FCC NaCl is formed in (TiZrNbTaHf)N layers, which are based on high-entropy alloy. In the WN layers, β-W_2N phases were observed (PDF 25-1257). All phases were oriented along (1 1 1), (2 0 0) and (3 1 1) directions in both samples (see Fig. 2). The similarity of structural states of different layers (relationship between the preferential orientations of crystallites formed in layers) indicates a correlation between the structures of the layers during their growth. With increasing of substrate bias from −90 V to −280 V, the general structural state of the coatings remains unchanged, however the peak intensities, and therefore their grain size, show important changes. For calculation of grain size, we used deconvolution of most intense peaks: (TiZrNbTaHf)N(1 1 1) and W_2N(1 1 1). In this case, the "error" will be full width at half maximum of peaks. The (TiZrNbTaHf)N(1 1 1) and W_2N(1 1 1) peaks have dramatically increased, with an associated grain size of τ = 15 ± 1 nm and τ = 12 ± 1 nm respectively, which contrasts with the values of −90 V sample, with τ = 4.5 ± 0.8 and τ = 2.7 ± 0.6 nm for (TiZrNbTaHf)N(1 1 1) and W_2N(1 1 1) respectively. Additionally, sample −280 clearly shows the apparition of (TiZrNbTaHf) (1 1 0) with a grain size of τ = 9.7 ± 0.6 nm with bcc crystal structure. The broad peaks at around ∼38° and ∼78° of the sample −280 V can be associated with precipitation of highly disordered bcc (1 1 0) and (2 2 0)-oriented high-entropy alloy phase. It is also worth noting that the application of high substrate bias leads to depletion of nitrogen in the coating, which coincides with the appearance of Me/Me chemical bonds. The literature is heavily populated with the scientific works, which indicate that the substrate bias play a decisive role on the growth processes of coatings. It was shown that, the application of high substrate bias leads to textural changes due to the enhanced mobility of deposited ions,

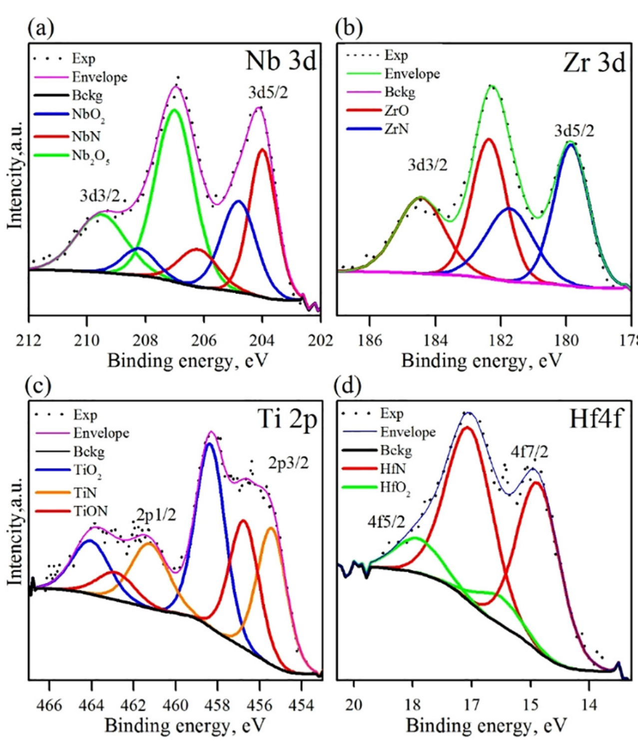

Fig. 1. XPS spectra of as-deposited (TiZrNbHfTa)N/WN multicomponent multilayer coating.

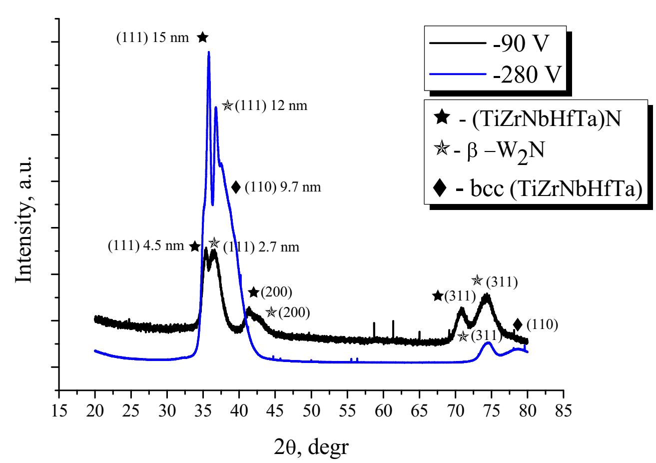

Fig. 2. Typical X-ray diffraction patterns of (TiZrNbHfTa)N/WN multicomponent multilayer coating depending on substrate bias.

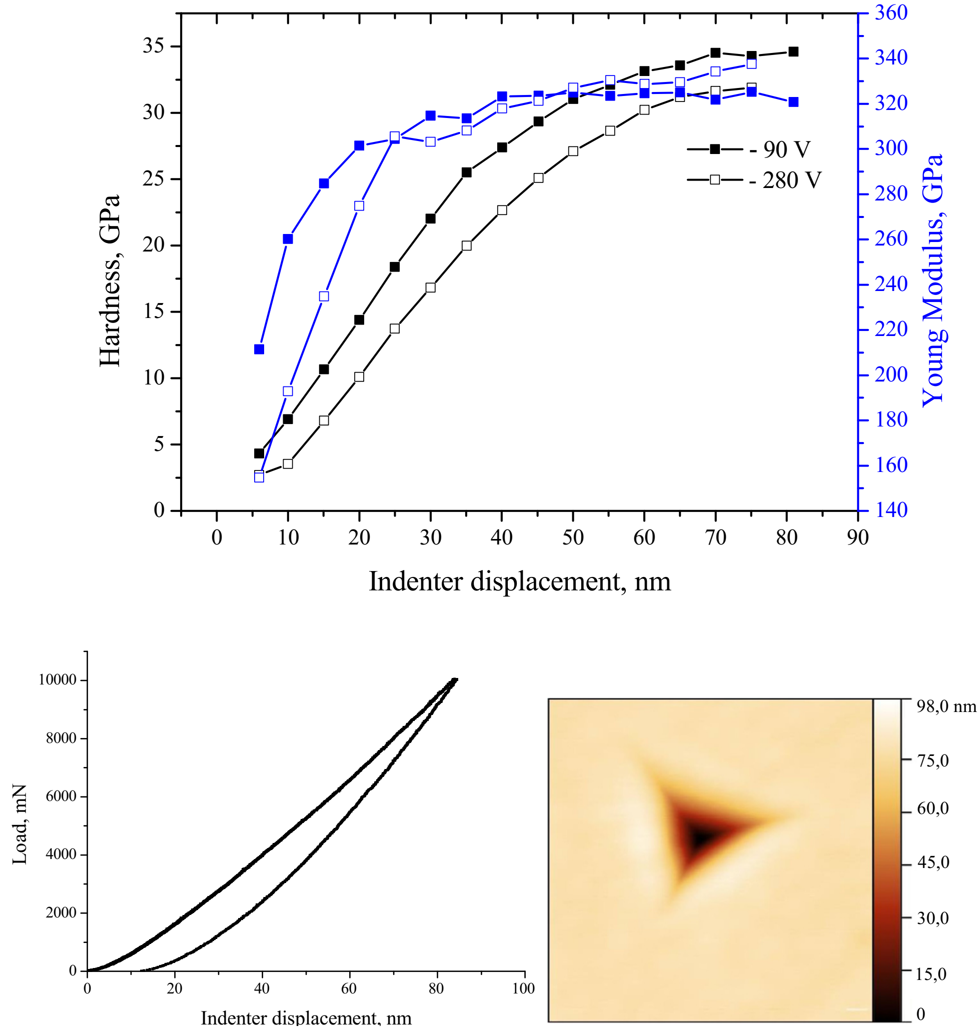

Fig. 3. Hardness and elastic modulus (a) of (TiZrNbHfTa)N/WN multilayer coatings vs. indenter displacement: −90 V and −280 V; b) load/unload – displacement curve; c) image of nanoindentation imprint.

anisotropy in surface diffusivities and different type of cascade effects [12–16].

The hardness and Young's modulus of the (TiZrNbHfTa)N/WN coating is 34 and 325 GPa at a substrate bias of −90 V (see Fig. 3). With increasing of substrate bias to −280 V, there is a slight decrease of hardness to 31 GPa and increase of Young's modulus to 337 GPa. Favorable chemical affinity of constituent elements towards nitrogen, formation of strong peaks from dense (1 1 1) plane, difference between mechanical properties of different layers, suppression of dislocation motion are the main reasons of high hardness of (TiZrNbHfTa)N/WN coatings. The possible explanation of decreasing of mechanical properties under high potential bias is annihilation of point defects and precipitation of relatively softer metallic bcc phase at the expense of reducing of nitrogen concentration. Also, the increment of grain size, observed from XRD, leads to a decrease in hardness according to the Hall-Petch relationship.

4. Conclusion

1. The formation of phases with cubic fcc crystal lattice in both layers of (TiZrNbTaHf)N/WN multilayer coatings is characteristic for all deposition regimes. The application of high substrate caused the increasing of the peak intensities of (TiZrNbTaHf)N (1 1 1) and W_2N(1 1 1), and precipitation of bcc metallic phase.
2. It was shown that mechanical properties of (TiZrNbTaHf)N/WN multilayer coatings are not highly depend on substrate bias. The hardness and Young's modulus of the (TiZrNbHfTa)N/WN coating is 34 and 325 GPa at a substrate bias of −90 V, 31 and 337 GPa – at −280 V.

Acknowledgements

Presented work was financially supported by Erasmus Mundus Eminence scholarship and by budget program "Multilayer and multicomponent coatings with adaptive behavior in wear and friction conditions" (No 0118U003579). A.P. gratefully acknowledge partial financial support from the National Science Centre of Poland within PRELUDIUM, under project number UMO-2015/19/N/ST5/01764.

References

[1] A.D. Pogrebnjak, A.A. Bagdasaryan, A. Pshyk, K. Dyadyura, Adaptive multicomponent nanocomposite coatings in surface engineering, Phys. Uspekhi 60 (2017) 586–607, https://doi.org/10.3367/UFNe.2016.12.038018.
[2] D.D. Kumar, N. Kumar, S. Kalaiselvam, S. Dash, R. Jayavel, Wear resistant super-hard multilayer transition metal-nitride coatings, Surfaces Interfaces 7 (2017) 74–82, https://doi.org/10.1016/j.surfin.2017.03.001.

[3] U. Helmersson, S. Todorova, S.A. Barnett, J.E. Sundgren, L.C. Markert, J.E. Greene, Growth of single-crystal TiN/VN strained-layer superlattices with extremely high mechanical hardness, J. Appl. Phys. 62 (1987) 481–484, https://doi.org/10.1063/1.339770.
[4] Y.Z. Tsai, J.G. Duh, Tribological behavior of CrN/WN multilayer coatings grown by ion-beam assisted deposition, Surf. Coatings Technol. 201 (2006) 4266–4272, https://doi.org/10.1016/j.surfcoat.2006.08.078.
[5] Y.Y. Chang, H. Chang, L.J. Jhao, C.C. Chuang, Tribological and mechanical properties of multilayered TiVN/TiSiN coatings synthesized by cathodic arc evaporation, Surf. Coatings Technol. (2018), https://doi.org/10.1016/j.surfcoat.2018.02.040.
[6] A.D. Pogrebnjak, V.I. Ivashchenko, P.L. Skrynskyy, O.V. Bondar, P. Konarski, K. Załęski, S. Jurga, E. Coy, Experimental and theoretical studies of the physicochemical and mechanical properties of multi-layered TiN/SiC films: Temperature effects on the nanocomposite structure, Compos. Part B Eng. 142 (2018) 85–94, https://doi.org/10.1016/j.compositesb.2018.01.004.
[7] E. Coy, L. Yate, Z. Kabacińska, M. Jancelewicz, S. Jurga, I. Iatsunskyi, Topographic reconstruction and mechanical analysis of atomic layer deposited Al_2O_3/TiO_2 nanolaminates by nanoindentation, Mater. Des. 111 (2016) 584–591, https://doi.org/10.1016/j.matdes.2016.09.030.
[8] A.V. Naumkin, A. Kraut-Vass, S.W. Gaarenstroom, C.J. Powell, NIST Standard Reference Database, 20, 2012.
[9] I. Milošev, H.-H. Strehblow, B. Navinšek, Comparison of TiN, ZrN and CrN hard nitride coatings: electrochemical and thermal oxidation, Thin Solid Films 303 (1997) 246–254, https://doi.org/10.1016/S0040-6090(97)00069-2.
[10] N. Jiang, H.J. Zhang, S.N. Bao, Y.G. Shen, Z.F. Zhou, XPS study for reactively sputtered titanium nitride thin films deposited under different substrate bias, Phys. B Condens. Matter. 352 (2004) 118–126, https://doi.org/10.1016/j.physb.2004.07.001.
[11] A.J. Perry, L. Schlapbach, An XPS study of hafnium nitride films, Solid State Commun. 56 (1985) 837–841, https://doi.org/10.1016/0038-1098(85)90416-8.
[12] A.D. Pogrebnjak, A.A. Bagdasaryan, V.M. Beresnev, U.S. Nyemchenko, V.I. Ivashchenko, Y.O. Kravchenko, Z.H.K. Shaimardanov, S.V. Plotnikov, O. Maksakova, The effects of Cr and Si additions and deposition conditions on the structure and properties of the (Zr-Ti-Nb)N coatings, Ceram. Int. 43 (2017) 771–782, https://doi.org/10.1016/j.ceramint.2016.10.008.
[13] G. Abadias, Stress and preferred orientation in nitride-based PVD coatings, Surf. Coatings Technol. 202 (2008) 2223–2235, https://doi.org/10.1016/j.surfcoat.2007.08.029.
[14] A.A. Bagdasaryan, A.V. Pshyk, L.E. Coy, P. Konarski, M. Misnik, V.I. Ivashchenko, M. Kempiński, N.R. Mediukh, A.D. Pogrebnjak, V.M. Beresnev, S. Jurga, A new type of (TiZrNbTaHf)N/MoN nanocomposite coating: microstructure and properties depending on energy of incident ions, Compos. Part B Eng. 146 (2018) 132–144, https://doi.org/10.1016/j.compositesb.2018.04.015.
[15] K.V. Smyrnova, A.A. Demianenko, A.S. Radko, A.V. Pshyk, O.V. Kuzovlev, H. Amekura, K. Oyoshi, Y. Takeda, The influence of the ion implantation of au- to the microstructure of the amorphous-nanocrystaline AlN-TiB2-TiSi2, J. Nano-Electron. Phys. 7 (2015) 1–5.
[16] I.A. Svito, A.K. Fedotov, A. Saad, P. Zukowski, T.N. Koltunowicz, Influence of oxide matrix on electron transport in (FeCoZr)x(Al2O3)1–x nanocomposite films, J. Alloys Compd. 699 (2017) 818–823, https://doi.org/10.1016/j.jallcom.2017.01.043.

Structural and mechanical characterization of (TiZrNbHfTa)N/WN multilayered nitride coatings [Текст] / A.A. Bagdasaryan, A.V. Pshyk, L.E. Coy [та ін.] // Materials Letters. — 2018. — №229. — С. 364-367.